Department of Physics (a) and Department of Chemical Engineering (b),
University of Florida, Gainesville [1]), and
Institute of Inorganic Chemistry, Russian Academy of Sciences, Novosibirsk [2]) (c)

Raman Scattering in Single-Crystal $GdBa_2Cu_3O_{7-\delta}$

By

V. Železný [3]) (a), D. B. Tanner (a), C. Park (b),
T. J. Anderson (b), L. P. Kozeeva (c), and A. A. Pavlyuk (c)

We report here on Raman spectra of the high-T_c superconductor material $GdBa_2Cu_3O_{7-\delta}$ (GBCO). GBCO is isomorphic with $YBa_2Cu_3O_{7-\delta}$ (YBCO), differing only in the substitution of Gd for Y. Thus, the group analysis performed for YBCO [1 to 3] is also applicable to GBCO. Orthorhombic GBCO belongs to the space group D_{2h} (Pmmm), with one molecular unit in the unit cell. We use the conventional structural notation [4] where the b-axis oriented chains contain Cu(1)–O(1) and superconducting planes Cu(2)–O(2)–O(3). In this structure the atoms occupy sites of the following symmetry: D_{2h} Y, Cu(1), and O(4); C_{2v} Ba, Cu(2), O(1), O(2), and O(3). The thirteen atoms in the unit cell yield a total of 39 degrees of freedom which can be classified by irreducible representations. At $k = 0$ (the center of Brillouin zone) group theory gives 15 Raman active vibrational modes: 5 A_g, 5 B_{2g}, and 5 B_{3g}. Raman scattering from the A_g modes can be observed in xx, yy, or zz geometries, whereas Raman scattering from the B_{2g} and B_{3g} modes is allowed in xz, zx, yz, and zy geometries. A summary of the vibrational modes in YBCO is presented in Table 1.

The five A_g phonons can be approximately attributed to the following motions [5, 6] all involving atomic motion along the c-axis of the unit cell: 500 cm^{-1}, stretching of the Cu(1)–O(4) bond; 435 cm^{-1}, O(2)–Cu(2)–O(3) bond bending, with the O(2) and O(3) moving in phase; 335 cm^{-1}, O(2)–Cu(2)–O(3) bond bending, with O(2) and O(3) moving out of phase; 145 cm^{-1}, Cu(2) motion; and 115 cm^{-1}, Ba motion.

Most of the measurements were performed on an extremely large ($5 \times 4 \times 1.5$ mm^3) GBCO crystal. The GBCO crystals were grown from a high-temperature melt of 0.7% Gd_2O_3, 29% BaO, and 70% CuO. This mixture was heated in an alumina crucible to 1060 °C for 5 h and then cooled at a rate of 10 K/day to 940 °C. The remaining liquid was decanted while still in the oven, to reduce the thermal stress in the crystals. The crystals were then cooled to room temperature at a rate of 10 to 20 K/h. Elemental analysis showed that the crystals contained a considerable amount of Al, presumably from dissolution of the crucible; the composition was found to be $GdBa_{1.8}Cu_{2.5}Al_{0.25}O_{7-\delta}$. Details of the growth of these crystals will be presented elsewhere [7]. The crystal size allowed measurement of both Raman and IR polarized reflectance spectra along the c-crystallographic axis. In addition, GBCO crystals were characterized by temperature dependent dc resistance and magnetic susceptibility measurements.

[1]) Gainesville, Florida 32611, USA.
[2]) Novosibirsk 630090, Russia.
[3]) Permanent address: Institute of Physics, CSAV, Prague 18040, Czech Republic.

Table 1

Summary of vibrational modes in YBCO

D_{2h}	number of acoustic modes	number of optical modes	activity	axis	atoms involved	trans- formation properties
A_g		5	Raman	c	Ba + Cu(2) + O(2) + O(3) + O(4)	x^2, y^2, z^2
B_{1g}			none			R_z, xy
B_{2g}		5	Raman	b	Ba + Cu(2) + O(2) + O(3) + O(4)	R_y, xz
B_{3g}		5	Raman	a	Ba + Cu(2) + O(2) + O(3) + O(4)	R_x, yz
A_u			silent		none	
B_{1u}	1	7	IR	c	Y + Ba + Cu(1) + Cu(2) + O(1) + O(2) + O(3) + O(4)	z
B_{2u}	1	7	IR	b	Y + Ba + Cu(1) + Cu(2) + O(1) + O(2) + O(3) + O(4)	y
B_{3u}	1	7	IR	a	Y + Ba + Cu(1) + Cu(2) + O(1) + O(2) + O(3) + O(4)	x
total	3	36	21 IR 15 Raman			

All Raman measurements were recorded at room temperature using a Jobin Yvon Ramanor U-1000 spectrometer equipped with a microprobe apparatus. The system was configured to collect the signal in an 180° backscattering geometry. Objective lenses of magnification 100× projected the laser beam onto a spot approximately 27 μm in diameter. Sample excitation was provided by an Innova-90-5 argon laser at a wavelength 514.5 nm with an excitation filter to suppress plasma lines. The laser power incident on the sample was about 10 mW and instrumental resolution was less than 3 cm^{-1}. Data accumulation times varied between 3 and 10 h depending upon the strength of the signal. The polarized IR reflectance was measured with a Bruker IFS 113v spectrometer over 100 to 4000 cm^{-1} (12 to 500 meV) and with a grating spectrometer over 200 to 40000 cm^{-1} (250 meV to 5 eV). Standard four-point probe techniques were used to measure the temperature dependence of the dc resistivity. The magnetic susceptibility was measured with a CTI squid magnetometer.

Observation of GBCO crystals under a polarizing microscope revealed a high density of ab-plane microtwins. As a result no distinction between the a- and b-axes could be made and the components of the Raman tensor α_{xx} and α_{xy} could be determined independently. The temperature dependence of the dc resistance showed two drops: one partial at 90 K and a second to zero resistance at 30 K. This result is believed to be caused by oxygen concentration variations in the sample. Control of the oxygen concentration during crystal growth from large charges is difficult because the oxygen diffusion length at growth temperature is smaller than the dimensions of the crystal.
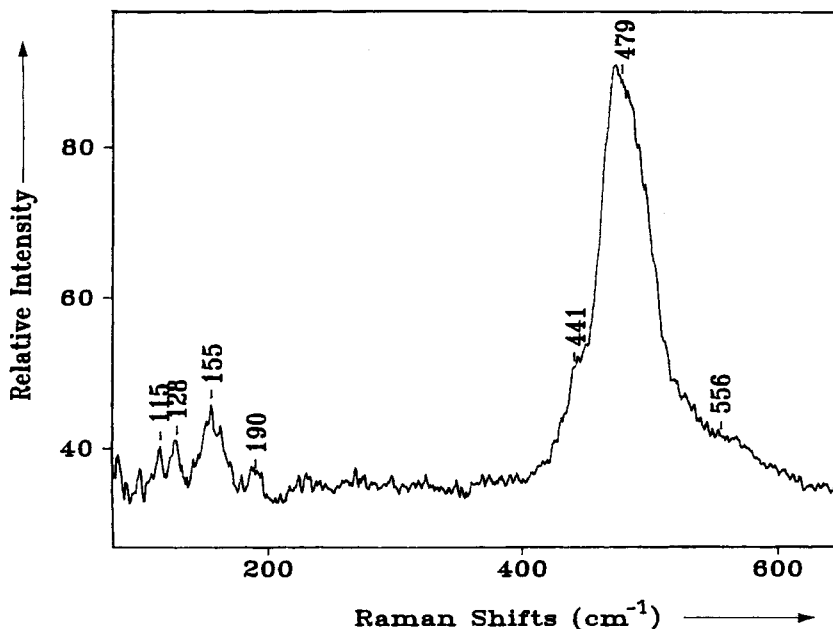
Fig. 1. Raman spectrum of A_g modes for $x(zz)\bar{x}$ or $y(zz)\bar{y}$ geometry

The temperature dependence of the magnetic susceptibility was well described by a Curie law, corresponding to the paramagnetic state produced by the uncompensated electron of Gd^{3+}. A small deviation from this $1/T$ dependence was observed at 87 K, possibly associated with the onset of superconducting diamagnetism.

The IR reflectance spectra showed a large anisotropy between polarization along the *ab* plane and perpendicular to it (*c*-axis) [8]. Our *ab*-plane data closely matched the spectra of Orenstein et al. [9], for a sample with $T_c = 30$ K. This is in agreement with the estimate of $T_c = 30$ K from dc resistance.

Raman spectra were recorded at room temperature perpendicular and parallel to the *c*-axis of the sample. Fig. 1 shows the scattering spectrum from a $x(zz)x$ or $y(zz)y$ geometry. The notion used here describes both the direction of travel and the plane of polarization of the incident and scattered light. $x(yy)x$ means that the incident light travels along the *a*-axis and is polarized parallel to *c*; the scattered light travels along *a* and is polarized to *c*. Because of twinning, the $x(zz)x$ and $y(zz)y$ geometries could not be distinguished. The most prominent feature is the strong peak at 480 cm^{-1}, while other maxima are located at 115, 128, 155, 440, and 556 cm^{-1}. A precise determination of the position of the high-frequency peaks was obtained by fitting the peaks to a Lorentzian function, with the estimated parameter given in Table 2.

Fig. 2 presents the spectrum for the $x(yy)x$ ($= y(xx)y$) geometry. The dominant peak in this spectrum was positioned at 335 cm^{-1}, while weaker peaks were observed at 115, 140, 190, and 230 cm^{-1}. An attempt was made to observe the B_{2g} and B_{3g} modes in the configurations (xz) and (yz) but no peaks were detected, presumably because of their low density.

As indicated previously, Raman spectra of GBCO should show five A_g modes at approximately the same frequencies as found in YBCO [10, 11]. This similarity in vibrational

Table 2

Fitted Lorentzian parameter values for the x(zz)x Raman spectrum

center (cm^{-1})	width (cm^{-1})	area
441	3	15
479	45	3700
556	52	210

frequencies is expected since the same atoms (Cu, O, Ba) are involved in the A_g modes of both YBCO and GBCO. The Y or Gd atoms do not directly contribute to the Raman spectrum, only shifting the frequencies slightly from anharmonic effects. A summary of the modes observed in this study is given in Table 3. The effect of incident polarization on the observed scattering intensities of the 335 cm^{-1} phonon and the other A_g phonons confirms that our sample was of good crystalline quality. Weak peaks observed in Fig. 1 and 2 at 128, 140, 190, and 230 cm^{-1} are similar to those in YBCO that have already been reported in literature [12]. It is believed that these peaks originate from extended defects or tetragonal domains partially present in the crystal. The broad band with maximum at 556 cm^{-1} is thought to be related to disorder on the oxygen chains [12].

Comparing the spectra recorded in this study with those reported by Krol et al. [13], it is clear that the spectra of this study are more nearly matched to the recent YBCO spectra. Most obviously, the band at 4800 cm^{-1} is substantially enhanced. The low-frequency phonons shown in Fig. 1 are much less pronounced than in YBCO [5, 14], particularly the
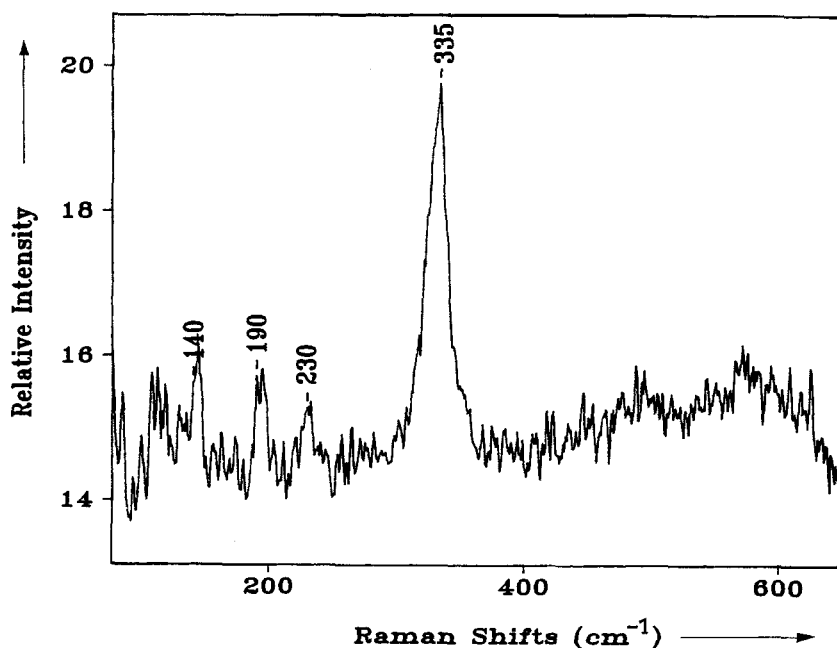

Fig. 2. Raman spectrum of A_g modes for $x(yy)\bar{x}$ or $y(xx)\bar{y}$ geometry

Table 3

Raman active modes GBCO and YBCO

crystal	GBCO	YBCO[a]	GBCO	YBCO[a]	GBCO	GBCO
symmetry	A_g	A_g	A_g	A_g	defects	defects
	$x(zz)\bar{x}$	$x(zz)\bar{x}$	$y(zz)\bar{y}$	$y(xx)\bar{y}$	$x(zz)\bar{x}$	$y(xx)\bar{y}$
	$y(zz)\bar{y}$	$y(zz)\bar{y}$	$x(yy)\bar{x}$	$x(yy)\bar{x}$	$y(zz)\bar{y}$	$x(yy)\bar{x}$
	115	115				
					128	
						140
frequency (cm^{-1})	115	145				
					190	190
						230
			335	335		
	441	435				
	479	470 to 500[b]			556	

[a] [1].

[b] Mode is sensitive to oxygen content. See [13].

intensity of the 115 cm^{-1} phonon in the *ab* plane. The spectrum shown in Fig. 2 is similar to the $y(xx)y$ one for YBCO and suggests a low density of twins in the near surface region where scattering occurred. Unfortunately, the crystal examined in this study did not have a second well developed surface perpendicular to the *ab* plane to verify this suggestion.

Raman spectroscopy has proven to be a sensitive technique for estimating the oxygen content in high-T_c superconductors. It has been shown [13] that the position of the peak produced by the stretching Cu(1)–O(4) bond shifts from 470 to 500 cm^{-1} as the stoichiometry changes from $YBa-2 Cu_3O_6$ to $YBa_2Cu_3O_7$. Assuming that the effect of the stoichiometry variation in GBCO on the position of this peak is the same as in YBCO, the oxygen concentration in our samples is estimated to be $GdBa_2Cu_3O_{6.4}$. This composition suggests that the crystal examined in this study lies in the vicinity of the metal–insulator phase transition on the metallic side of the solidus for this phase transition. A recent study [12] determined the composition of this phase transition to be $O_{6.35}$. Thus, the crystal under examination is expected to be a superconductor with T_c near 30 K. This expectation is supported by the dc conductivity measurement and infrared data described earlier.

In summary, the Raman spectra of GBCO are very similar to that of YBCO. The substitution of the much heavier Gd has a minimal effect on the frequencies of the A_g modes, because Gd does not participate directly in the normal modes. The principal effect seems to be a hardening of the Cu(2) motion and of the O(2)–Cu(2)–O(3) bond bending.

References

[1] R. FEILE, Physica **159C**, 1 (1989).

[2] C. THOMSEN and M. CARDONA, in: Physical Properties of High-T_c Superconductors, Ed. D. M. GINSBERG, World Scientific, Singapore 1989 (p. 410).

[3] G. BURNS, F. H. DACOL, and P. FREITAS, Solid State Commun. **64**, 471 (1987).

[4] J. D. JORGENSEN, M. A. BENO, D. G. HINKS, L. SODERHOLM, K. J. VOLIN, R. L. HITTERMAN, J. D. GRACE, I. K. SCHULLER, C. U. SEGRE, K. ZHANG, and M. S. KLEEFISH, Phys. Rev. B **36**, 3608 (1987).

[5] K. F. McCarty, J. Z. Liu, R. N. Shelton, and H. B. Radousky, Phys. Rev. B 41, 8792 (1990).

[6] M. Stavola, D. M. Krol, W. Weber, S. A. Sunshine, A. Jayraman, G. A. Kourouklis, R. J. Cava, and E. A. Rietman, Phys. Rev. B 36, 850 (1987).

[7] L. P. Kozeeva and A. A. Pavlyuk, private communication.

[8] V. Železný, D. B. Tanner, and K. Kamarás, Bull. Amer. Phys. Soc. 36, 418 (1991).

[9] J. Orenstein, G. A. Thomas, A. J. Millis, S. L. Cooper, D. H. Rapkine, T. Timusk, L. F. Schneemeyer, and J. V. Warszak, Phys. Rev. B 42, 6342 (1990).

[10] C. Thomsen, M. Cardona, W. Kreiss, R. Liu, L. Genzel, M. Bauer, and U. Schroder, Solid State Commun. 65, 1139 (1989).

[11] R. Liu, C. Thomsen, W. Kress, M. Cardona, B. Gegenheimer, F. W. de Wette, J. Prade, and A. D. Kulkarni, Phys. Rev. B 36, 7971 (1988).

[12] G. Burns, F. H. Dacol, C. Feild, and F. Holtzberg, Solid State Commun. 77, 367 (1991).

[13] D. M. Krol, M. Stavola, W. Weber, L. F. Schneemeyer, J. V. Warszak, S. M. Zahurak, and S. G. Kosinski, Phys. Rev. B 36, 8325 (1987).

[14] F. Slakey, S. L. Cooper, M. V. Klein, J. P. Rice, and D. M. Ginsberg, Phys. Rev. B 39, 2781 (1989).